UNIVERSITY OF MINNESOTA

Twin Cities Campus

Saint Anthony Falls Laboratory
Engineering, Environmental, Biological and Geophysical Fluid Dynamics

College of Science and Engineering

Mississippi River at 3rd Avenue S.E.
Minneapolis, MN 55414

Dept. Main Office: 612-624-4363
Fax: 612-624-4398

Project Title: Development of a High-Resolution Virtual Wind Simulator for Optimal Design of Wind Energy Projects

Contract Number: RD3-42 **Milestone Number: 6** **Report Date:** 06/28/12

Principal Investigator: Fotis Sotiropoulos **Contract Contact:** Bridget Foss

fotis@umn.edu 612-624-5571

Congressional District: (Corporate office) Minnesota 5th

Congressional District: (Project location) Minnesota 5th

MILESTONE REPORT

Executive Summary:

This project aims at developing a '*Virtual Wind Simulator*' (VWS) for the prediction of atmospheric boundary layer flow and its interactions with wind turbines and wind farms. The use of the simulator will assist in the improved design of potential wind energy projects by providing more accurate predictions of local and wind turbulence at site and turbine levels. Additionally, the VWS will help increase the level of wind energy utilization and reduce the cost of energy production.

Computational Fluid Dynamics (CFD) methods are used in this project to develop a computational framework for conducting high-resolution simulations of wind turbulence at the meso and micro scales. In particular, the Large-Eddy Simulation (LES) technique will allow for accurate simulations of the turbulent flow at spatial resolutions as small as one to ten meters, and temporal resolutions of just a few seconds. Parameterizations for wind turbine forces will also be developed in the LES framework. In addition, three-dimensional, time-evolving flow fields obtained from LES at any location within a potential wind farm site could then be used as the inflow condition for even more detailed simulations of the turbulent flow around the blades of specific wind turbines using a hybrid Reynolds-Averaged Navier-Stokes (RANS)/LES technique. The SAFL computational models will be coupled to macro-scale regional models to develop a powerful multi-scale computational tool, the VWS. The VWS will integrate the latest advancements in computational fluid dynamics research and provide reliable, high-resolution descriptions of wind turbulence across the entire range of scales that are relevant to wind power production. This information will provide objective, scientifically

based criteria that can be used by wind energy project developers for the site-specific, optimal selection and placement (micro-siting) of wind turbines.

As planned, during this reporting period (quarter) activities have been carried out that address the following objectives:
(a) The computational fluid dynamics (CFD) framework for accurate simulation of high-resolution wind and turbulence fields and their effects on wind turbine operation and energy output is completed.
(b) Validation of the proposed *Virtual Wind Simulator* using high-resolution wind and turbulence measurements collected in an atmospheric boundary layer wind tunnel is completed.
(c) Weather Research and Forecast (WRF) model was used to assess the ability of the model to characterize the wind in an operating wind farm when turbines are operating. Analysis of the simulation and comparison with field data is ongoing.

Project funding provided by customers of Xcel Energy through a grant from the Renewable Development Fund.

Technical Progress:
We have made substantial progress in Task 1, Task 2 and Task 4. The progress made in the three tasks is discussed below.

Task 1. Development of the *Virtual Wind Simulator* for high-resolution simulations of wind turbulence and their effect on energy production

Virtual Wind Simulator – High resolution model
The Virtual Wind Simulator employs large-eddy simulation (LES) for the wind field and actuator disk/line model for parameterizing the wind turbine rotors. The governing equations are filtered Navier-Stokes equations, which are discretized using second-order accurate, three-point central finite-differencing for all spatial derivatives. The discrete equations are integrated in time using the second-order accurate fractional step method. An algebraic multigrid acceleration along with GMRES solver is used to solve the pressure Poisson equation and matrix-free Newton-Krylov method is used for the filtered momentum equation. A dynamic subgrid scale model is used in LES for the small scales.
For the actuator disk model, the wind turbine rotor is represented by a permeable disk as shown in left plot of Fig.1. The forces are uniformly distributed on the disk for actuator disk model, in which the thrust force coefficient is from the one-dimensional momentum theory, which is shown as follows:

$$C_T = 4a(1-a),$$

where a is the induction factor. For the actuator line model, the rotor blade is represented by a single line as shown in left plot of Fig.1. The drag and lift coefficients are obtained from a look-up table. The mesh for the actuator disk/line model generally does not coincide with the background mesh for the fluid. A regularized delta function is used to transfer the quantities between the two meshes.

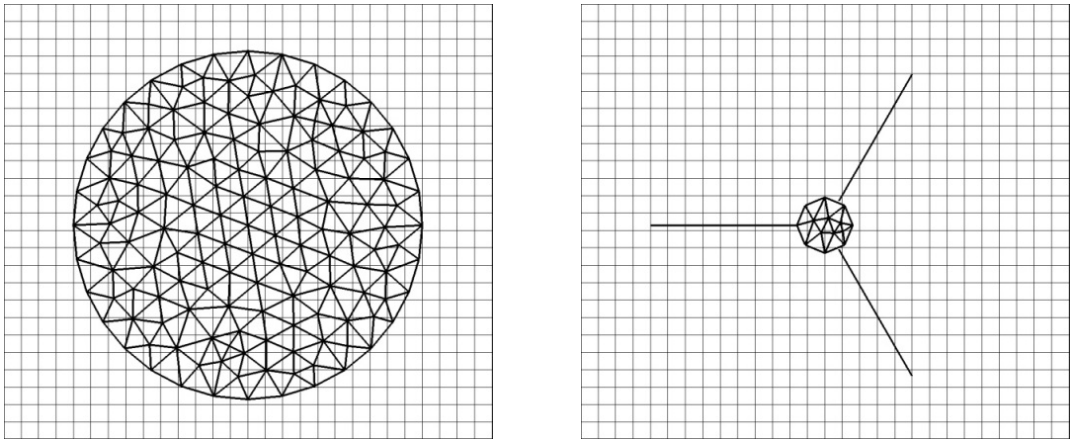

Figure 1: Schematic of the meshes used for actuator disk model (left) and actuator line model (right).

Virtual Wind Simulator – weather model for large-scale wind patterns

A simulation was conducted with the Weather Research and Forecast (WRF) model to assess the ability of the model to characterize the wind in an operating wind farm when the turbines are operating. For the simulation, we chose a time period of several days during the field measurement period when the wind direction was relatively steady from the south and the atmospheric boundary layer conditions varied from convective (daytime) stable (nocturnal). During this time period, the sodars were able to measure several instances of waking in the southernmost row of turbines during periods of both convective and stable boundary layer conditions. Thus, this time period provides the best opportunity for comparisons between models and the sodar and the turbine data.

The period of modeling started July 1, 2010 at 0000 UTC and ended July 5, 2010 at 0000 UTC. The WRF outermost domain had a grid interval of 13.5 km, and its initial and lateral boundary conditions were provided from global forecast system (GFS) model analyses (for 0000, 0600, 1200, and 1800 UTC) and 3-hour forecasts (for 0300, 0900, 1500, and 2100 UTC). Two-way nesting was used for the inner domains, which had grid intervals of 4.5 km, 1.5 km, and 500 meters. The innermost grid encompassed the Mower County wind farm and neighboring wind farms to the south and north.

The latest version of WRF has a wind turbine parameterization that can be utilized to predict the effects of wind power generation on the atmospheric flow. For this particular run, we modified the wind turbine parameterization to employ the turbine thrust coefficients specific to the Siemens 2.3 MW turbines operating at the Mower County wind farm. The turbines were assumed to be operating during the entire model run period. For the neighboring wind farms, there was no data available regarding the specific turbines or their thrust coefficients, but the locations of individual turbines within these wind farms could be determined using Google Earth ™. To provide at least a rough estimate of the operation of these surrounding farms, the farms were assumed to have General Electric SLE 1.5 MW turbines.

The analysis of this run is ongoing. The WRF output wind speeds will be compared with supervisory control and data acquisition (SCADA) system data from the wind turbines

every 10 minutes. Likewise, the WRF data can also be compared with SODAR observations taken in the southwestern segment in the farm and in the northernmost row of turbines. Fig. 2 shows a snapshot of the WRF output wind speeds and direction. The turbine wakes are evident in the reduced wind speeds to the north of the operating turbines in the farm with a particularly sharp contrast in the southernmost half of the farm. Due to the available grid interval in WRF, the gradients of wind speed are not nearly as sharp as are observed in the wind farm, and the turbine wakes are artificially wide compared to the individual turbine wakes, particularly in the near field region (less than 10 rotor diameters downstream). In particular, Turbine 42 sees a sharper reduction in wind speed than is predicted in WRF. Wind speeds for this particular time are also less at turbines 32-38, 25-27, 12-14, 2-6, and 9-11 than predicted by WRF. The variability of the wind at these spatial scales is not captured by the 500 meter grid interval of the innermost domain.

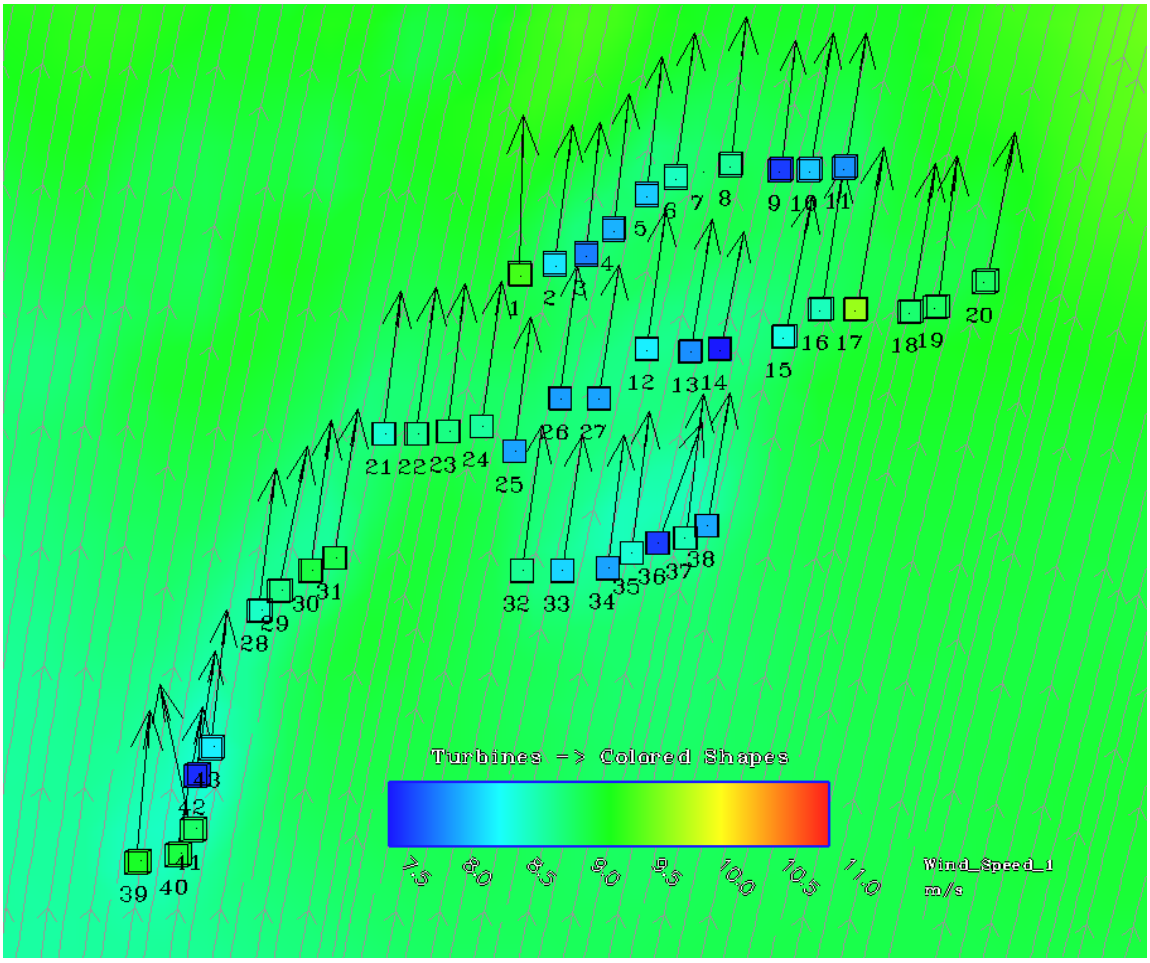

Figure 2: WRF model wind speed at 80 meters AGL (colored shading), wind speed measured by the wind turbine SCADA system (colored shapes), streamlines on the 80 meter AGL surface, and SCADA wind vectors (arrows) at 1440 UTC July 3, 2010.

Task 2. Validation of the *Virtual Wind Simulator* using wind tunnel measurements

The actuator disk/line model is first validated for a single wind turbine. Numerical simulation is compared with our wind tunnel experiment. As shown in the conceptual set-up of Fig. 3, the wind is from left to right. At the top, free slip and non-penetration boundary conditions are used for parallel and normal velocity components, respectively. At the ground, wall model is used. In the spanwise direction, a periodic boundary condition is employed. At the inflow plane, velocity profiles are provided by additional simulation of turbulent channel flows. At the outflow plane, Neumann boundary condition is used.

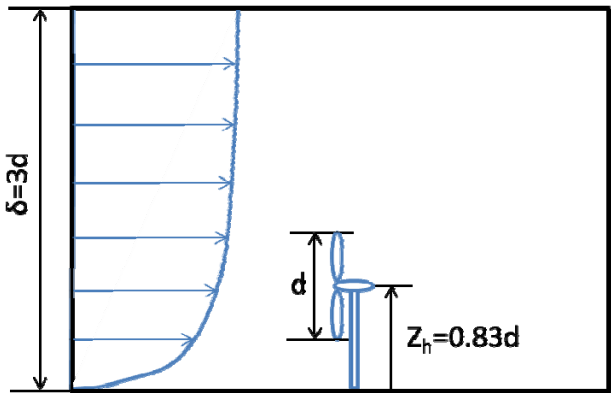

Figure 3: Schematic for one turbine case.

The comparison of the inflow velocity boundary conditions with the wind tunnel case is shown in Fig. 4. The inflow conditions used in the present LES show good agreements with that obtained from the wind tunnel.

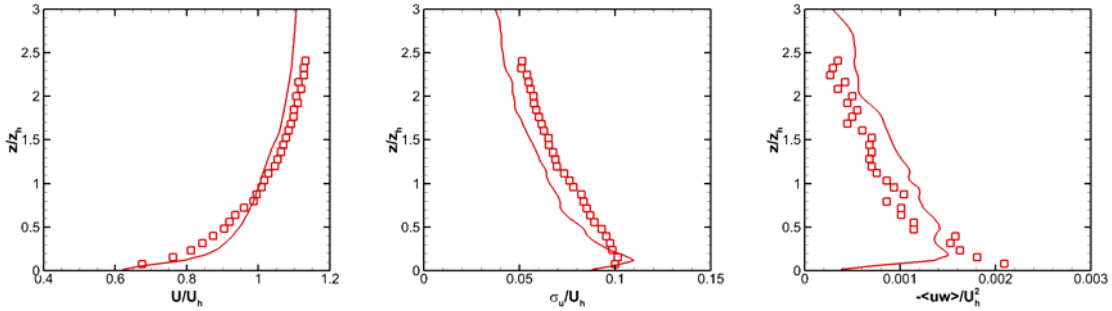

Figure 4: Comparison of inflow conditions used in LES with wind tunnel experiment. Lines: LES; square symbols: experiment. Left: mean velocity profile; middle: streamwise turbulence intensity; right: Reynolds shear stress.

The comparison of mean velocity profiles in the turbine wake at various locations in its symmetry plane is shown in Fig. 5. Results from the actuator line model agree well with the wind tunnel experiment at all locations. The actuator disk model shows good agreement with experiment in the far wake (5D and 10D), but some discrepancies are observed in the near wake (2D).

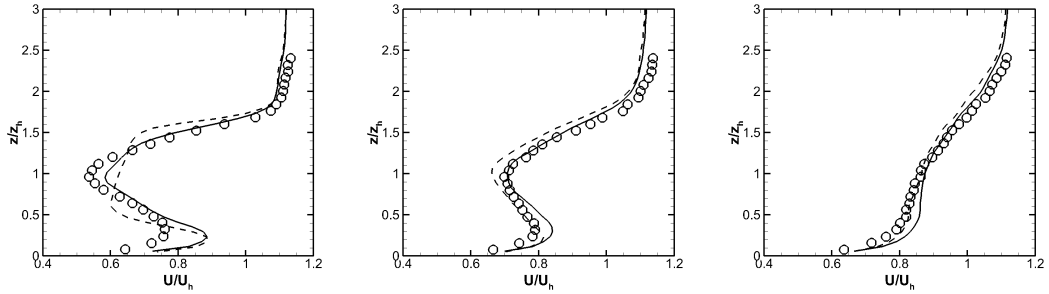

Figure 5: Comparison of mean velocity profiles at different downstream locations. From left to right: 2D, 5D and 10D. Symbols: experiment; solid line: actuator line model; dashed line: actuator disk model.

In Fig. 6, we compare the turbulence intensity in the wake at the same locations given in the mean velocity profiles of Fig. 5. Similar levels of agreements are observed. The prediction of the actuator line model agrees very well with the predictions from experiments for all downstream locations. The actuator disk model, on the other hand, gives good predictions mainly in the far wake region.

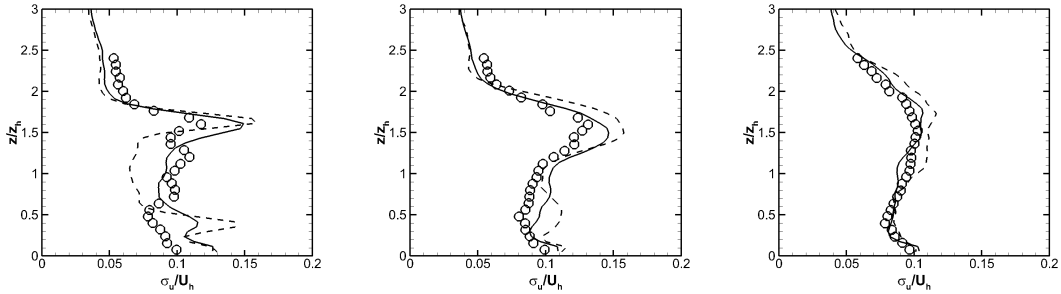

Figure 6: Comparison of streamwise turbulence intensities at different downstream locations. From left to right: 2D, 5D and 10D. Symbols: experiment; solid line: actuator line model; dashed line: actuator disk model.

Fig. 7 shows the comparison of the Reynolds shear stress with the wind tunnel experiment. At 2D downstream, the results from actuator line model show better agreements with the experimental results compared with the actuator disk model. For large downstream locations (5D and 10D), both actuator disk and actuator line models show good agreement with the wind tunnel experiment.

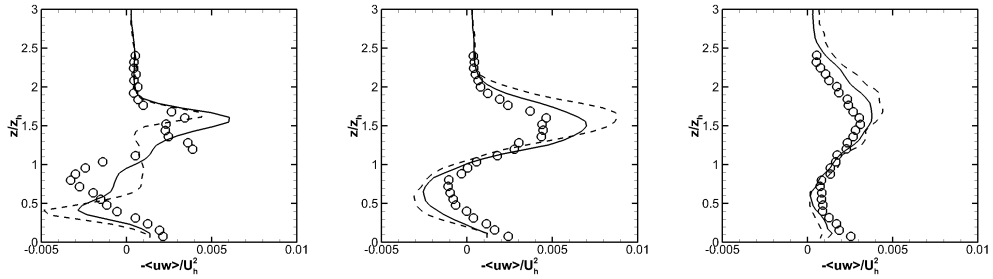

Figure7: Comparison of Reynolds shear stresses at different downstream locations. From left to right: 2D, 5D and 10D. Symbols: experiment; solid line: actuator line model; dashed line: actuator disk model.

In addition, the actuator disk model is further validated for infinite wind farm simulations. We employ the same layout of wind turbines with the reference (Calaf et al., Phys. Fluids, 22, 015110, 2010) as shown in Fig. 8. There are 4 turbines and 6 turbines in the streamwise (x) and spanwise directions (y). At the top, free slip boundary condition and non-penetration boundary conditions are used for parallel and normal velocity components, respectively. At the surface, wall model is used. Periodic boundary condition is used in horizontal directions. It should be noted, however, that there are some differences between our solver with that used in Calaf et al 2010. First, They employed a pseudospectral discretization in the horizontal directions and finite differencing in the vertical direction in order to solve the filtered Navier-Stokes equations, while we employ second-order accurate finite-differencing in all three directions. Second, the actuator disk model is implemented slightly differently in the two models. While Calaf et al. obtained the averaged velocity on the disk by using spatial and temporal averaging, we only use the spatial averaging. Finally, the subgrid scale models employed by Calaf et al. are the Lagrangian dynamic Smagorinsky model and the standard Smagorinsky model, while we employ the dynamic Smagorinsky model.

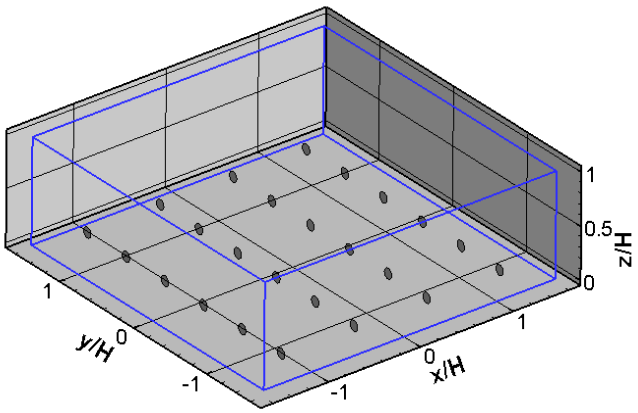

Figure 8: Schematic of the layout of wind turbines

In Fig. 9, we show the comparison of the present simulation with those from Calaf et al 2010. As seen, both the mean velocity profile and Reynolds and dispersive shear stresses show good agreements despite of the differences between the two solvers.

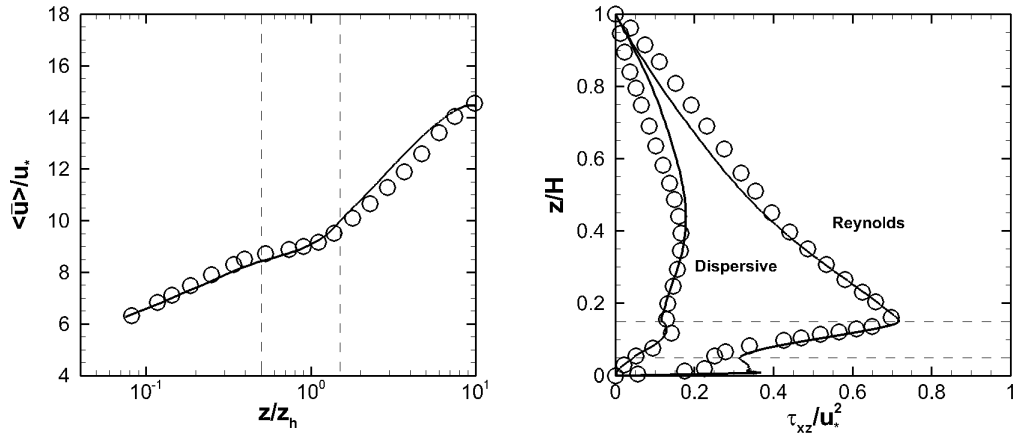

Figure 9: Comparison of the predictions from the present LES (with actuator model) and Calaf et al 2010. Symbols: Calaf et al; solid lines: present. Left: mean velocity profile; right: Reynolds and dispersive shear stresses.

In summary, the Virtual Wind Simulator (LES with actuator disk/line model) has been well validated for both one standing alone wind turbine case and infinite large wind farm cases by comparing the results from present model with the wind tunnel experiment and other researcher's numerical simulation in literature, respectively. Compare with actuator disk model, actuator line model gives better predictions for small downstream locations. For far wake locations, the predictions from both actuator disk and actuator line models are almost the same. While the resolution requirement for actuator disk model is lower for actuator disk model, so the actuator disk model is well suited for large wind farm simulations when high resolution is very expensive.

Task 4. Virtual wind simulator Application (Wind Assessment at Undeveloped Site with Complex Terrain)

Field experiments

The data from the second phase of the experiment have been archived, and we are presently using the data for detailed study, modeling, and model-data intercomparisons. One case was selected from the Mower County field experiment, which provided data for a case study under neutral atmospheric conditions. We are looking for cases with stable (nocturnal) boundary layer stratification to provide data for further modeling studies.

The second phase of the field experiment at Mower County wind farm began April 28, 2010 and continued until August 11, 2010. The two Triton sodars were deployed in the same location as in the first phase of the Mower field experiment between Turbines 39 and 40 and between Turbines 41 and 42 in the southwestern portion of the wind farm.

On May 19, two additional instruments were added to the field experiment. An Atmospheric Systems Corporation (ASC) sodar was installed between Turbines 8 and 9 in the northeastern portion of the wind farm. A ZephIR lidar was installed next to the ASC sodar to provide intercomparison data between the lidar and sodar. Together, the two additional instruments measured the accumulated wakes in the northernmost row of the wind farm (Turbines 1 through 11).

Additional Milestones:

Work is in progress towards Milestone 7.

Project Status:

The project is ahead of schedule due to the fact that work on the project started before the contract was finalized.

Appendix:

List publications

Papers in Refereed Journals

10. Yang X., Kang S. and Sotiropoulos F. 'Computational study and modeling of turbine spacing effects in infinite aligned wind farms'. *Under review* (comments received).
9. Chamorro, L.P., Arndt, REA and Sotiropoulos F. 'Drag reduction in large wind turbines through riblets: Evaluation of riblet geometry and application strategies'. *Renewable Energy*. *Under review* (comments not received).
8. Chamorro, L.P., Guala, M., Arndt, REA and Sotiropoulos F. 'On the evolution of turbulent scales in the wake of a wind turbine model'. *J. of Turbulence*. (accepted for publication on May 17, 2012. Currently under production).
7. Chamorro, L.P., Arndt, REA and Sotiropoulos F, 2011. 'Turbulent flow properties around a staggered wind farm'. *Bound. Layer Meteorol*. Vol 141-3: 349-367.
6. Chamorro, L.P., Arndt, REA and Sotiropoulos F, 2011. 'Reynolds number dependence of turbulence statistics in the wake of wind turbines'. *Wind Energy*. DOI: 10.1002/we.501.
5. Chamorro, L.P. and Arndt, REA. 2011. 'Non-uniform velocity distribution effect on the Betz limit' *Wind Energy*. DOI: 10.1002/we.549.
4. Chamorro, L.P., and F. Porté-Agel, 2010. 'Thermal stability and boundary-layer effects on wind turbine wakes. A wind tunnel study'. *Boundary-Layer Meteorology*, 136: 489-513.
3. Lu, H., and F. Porté-Agel, 2010. 'A modulated subgrid-scale model for large-eddy simulation: Application to a neutral atmospheric boundary layer'. *Physics of Fluids*, 22(1):015109.
2. Wu, Y.-T., and F. Porté-Agel, 2011. 'Large-eddy simulation of wind-turbine wakes: Evaluation of turbine parameterizations'. *Boundary-Layer Meteorology*, 138:345–366.
1. Chamorro, L.P., and F. Porté-Agel, 2009. 'A wind tunnel investigation of wind turbines wakes: Boundary-layer turbulence and surface roughness effects'. *Boundary-Layer Meteorology*, 132: 129-149.

Conference Presentations

13. Chamorro L.P., Arndt R.E.A., Yang X. and Sotiropoulos F. 2012. 'Characterization of the turbulent structure and transport processes in the wake of a wind turbine under different canonic configurations'. Euromech Colloquium 528, Oldenburg, Germany.
12. Yang X., Sotiropoulos F. 2011. 'LES investigation of turbine spacing effects in wind farms'. The 64th Annual Meeting of the American Physical Society, Baltimore, Maryland.
11. Chamorro L.P., Arndt R.E.A. and Sotiropoulos F. 2011. 'Turbine layout effects on the flow structure inside an above large wind farms'. American Physical Society, Baltimore, Maryland.
10. Chamorro, L.P., R.E.A. Arndt and F. Sotiropoulos, 2011. 'Turbulence patterns

around a large wind farm'. 49th AIAA Aerospace Sciences Meeting, Orlando, Florida.
9. Chamorro, L.P., R.E.A. Arndt and F. Sotiropoulos, 2010. 'Turbulence characteristics around a staggered wind farm configuration. A wind tunnel study'. American Physical Society Meeting. Minneapolis, Long Beach, CA.
8. Porté-Agel, F., Y.-T. Wu, and H. Lu, 2009. 'Large-eddy simulation of wind-turbine wakes'. American Physical Society Meeting. Minneapolis, MN.
7. Chamorro, L.P., and F. Porté-Agel, 2009. 'A wind tunnel investigation of wind turbine wakes'. American Physical Society Meeting. Minneapolis, MN.
6. Porté-Agel, F., F. Sotiropoulos, R. Conzemius, L. Chamorro, Y.-T. Wu, S. Behara, H. Lu, 2009. 'Development of a high-resolution Virtual Wind Simulator for optimal design of wind energy projects'. E3 -Energy, Economic and Environmental-Conference. Minneapolis, MN.
5. Porté-Agel, F., Y.-T. Wu, Y.-T.., H. Lu, 2009. 'Parameterization of turbulent fluxes and wind-turbine forces in large-eddy simulation'. European Geophysical Union. Vienna.
4. Chamorro, L.P., and F. Porté-Agel, 2009. 'A wind tunnel investigation of wind turbine wakes: Boundary-layer turbulence and surface roughness effects'. European Geophysical Union. Vienna.
3. Wu, Y.-T.., H. Lu, and F. Porté-Agel, 2008. 'Large-eddy simulation of wind-turbine wakes'. American Geophysical Union. San Francisco, CA.
2. Chamorro, L.P., and F. Porté-Agel, 2008. 'A wind tunnel investigation of wind turbine wakes: Boundary-layer turbulence and surface roughness effects'. American Geophysical Union. San Francisco, CA.
1. Porté-Agel, F., F. Sotiropoulos, R. Conzemius, L. Chamorro, Y.-T. Wu, S. Behara, H. Lu, 2008. 'Development of a high-resolution Virtual Wind Simulator for optimal design of wind energy projects'. E3 -Energy, Economic and Environmental-Conference. Minneapolis, MN.